AEDC-TR-81-23

Experimental Verification of an Aerodynamic Parameter Optimization Program for Wind Tunnel Testing

Richard L. Palko and Margaret Anne Crawford
Calspan Field Services, Inc.

November 1981

Final Report for Period October 1980 – September 1981

ARNOLD ENGINEERING DEVELOPMENT CENTER
ARNOLD AIR FORCE STATION, TENNESSEE
AIR FORCE SYSTEMS COMMAND
UNITED STATES AIR FORCE

APPROVAL STATEMENT

This report has been reviewed and approved.

ALVIN R. OBAL, Captain, CF
Directorate of Technology
Deputy for Operations

Approved for publication:

FOR THE COMMANDER

MARION L. LASTER
Director of Technology
Deputy for Operations

UNCLASSIFIED

SECURITY CLASSIFICATION OF THIS PAGE (When Data Entered)

REPORT DOCUMENTATION PAGE		READ INSTRUCTIONS BEFORE COMPLETING FORM
1. REPORT NUMBER AEDC-TR-81-23	2. GOVT ACCESSION NO.	3. RECIPIENT'S CATALOG NUMBER
4. TITLE (and Subtitle) EXPERIMENTAL VERIFICATION OF AN AERODYNAMIC PARAMETER OPTIMIZATION PROGRAM FOR WIND TUNNEL TESTING		5. TYPE OF REPORT & PERIOD COVERED Final Report, October 1980 - September 1981
		6. PERFORMING ORG. REPORT NUMBER
7. AUTHOR(s) Richard L. Palko and Margaret Anne Crawford, Calspan Field Services, Inc./AEDC Division		8. CONTRACT OR GRANT NUMBER(s)
9. PERFORMING ORGANIZATION NAME AND ADDRESS Arnold Engineering Development Center/DOT Air Force Systems Command Arnold Air Force Station, TN 37389		10. PROGRAM ELEMENT, PROJECT, TASK AREA & WORK UNIT NUMBERS Program Element 65807F
11. CONTROLLING OFFICE NAME AND ADDRESS Arnold Engineering Development Center/DOS Air Force Systems Command Arnold Air Force Station, TN 37389		12. REPORT DATE November 1981
		13. NUMBER OF PAGES 29
14. MONITORING AGENCY NAME & ADDRESS(if different from Controlling Office)		15. SECURITY CLASS. (of this report) UNCLASSIFIED
		15a. DECLASSIFICATION/DOWNGRADING SCHEDULE N/A

16. DISTRIBUTION STATEMENT (of this Report)

Approved for public release; distribution unlimited.

17. DISTRIBUTION STATEMENT (of the abstract entered in Block 20, if different from Report)

18. SUPPLEMENTARY NOTES

Available in Defense Technical Information Center (DTIC).

19. KEY WORDS (Continue on reverse side if necessary and identify by block number)

wind tunnel testing
aerodynamic parameters
optimization
algorithm

20. ABSTRACT (Continue on reverse side if necessary and identify by block number)

The optimization algorithm developed for the SOFT wing program has been revised to make it more applicable for use in routine wind tunnel testing. The algorithm modification removed some unused routines and simplified the control input requirements. The modified optimization algorithm was demonstrated in the 1-ft transonic Aerodynamic Wind Tunnel (1T) using a 3-degree-of-freedom model. The test Mach number was 0.8. The algorithm was successfully demonstrated for all three optimization runs attempted.

20. ABSTRACT, Concluded.

These included minimization of drag coefficient for a specified coefficient of lift, maximization of lift coefficient for a specified coefficient of drag, and maximization of lift-to-drag ratio for a specified coefficient of drag.

PREFACE

The work reported herein was conducted by the Arnold Engineering Development Center (AEDC), Air Force Systems Command (AFSC), at the request of the AEDC Directorate of Technology (DOT). The Air Force project manager was Capt. A. Obal (CF), AEDC/DOTR. The results of the research were obtained by Calspan Field Services, Inc., AEDC Division, operating contractor for Aerospace Flight Dynamics Testing at the AEDC, AFSC, Arnold Air Force Station, Tennessee, under Project Number P32C-B8. The manuscript was submitted for publication on September 15, 1981.

CONTENTS

ILLUSTRATIONS

TABLES

1.0 INTRODUCTION

From 1976 to 1979 a research program was conducted to develop the Self-Optimizing Flexible Technology (SOFT) wing (Refs. 1 through 3). The SOFT wing concept is that of a wing that automatically adapts its shape (through conformal variations of camber, twist, and leading-edge sharpness) to minimize or maximize various prescribed merit functions (e.g., minimum drag or maximum lift), subject to various constraints (e.g., fixed lift, trim, structural limits, etc). A semispan model representative of the F-111 TACT aircraft was used and contained 12 independently controllable hydraulic actuators in the wing (to conformally vary wing camber and twist) and one hydraulic tail actuator (to vary tail incidence). During this research effort the capability to optimize the wing shape for a minimum drag while maintaining a specified lift and pitching moment was successfully demonstrated. However, the limited testing time available during the program did not permit demonstration of optimization of any additional aerodynamic parameters.

The optimization algorithm used for the SOFT wing program was specifically developed for that program. Therefore, a follow-on study was conducted to revise the optimization algorithm to make it a more usable tool for general wind tunnel test application. The algorithm was streamlined by removing routines that were not used and generalized by changing the algorithm to accept information in the units of the control parameters (deg, psi, in., etc.) rather than in counts, as previously required. The new algorithm was verified in the 1-ft transonic Aerodynamic Wind Tunnel (1T) with a 3-degree-of-freedom model. Optimizations to minimize C_D for a specified C_L, to maximize C_L for a specified C_D, and to maximize L/D for a specified C_D were accomplished. The results obtained during operation and evaluation of the modified optimization algorithm are presented herein.

2.0 APPARATUS

2.1 TUNNEL 1T

Tunnel 1T is a continuous-flow, nonreturn, transonic wind tunnel equipped with a two-dimensional, flexible nozzle and a plenum evacuation system. The test section Mach number can be varied from 0.2 to 1.5. The tunnel is operated at a stagnation pressure of about 2,850 psfa with a ±5-percent variation depending on the tunnel resistance and the ambient conditions. Stagnation temperature can be varied from 80 to 120°F above ambient temperature when necessary to prevent moisture condensation in the test region. A schematic of the tunnel and its associated equipment is shown in Fig. 1. Additional details on the tunnel and its associated equipment are presented in Ref. 4.

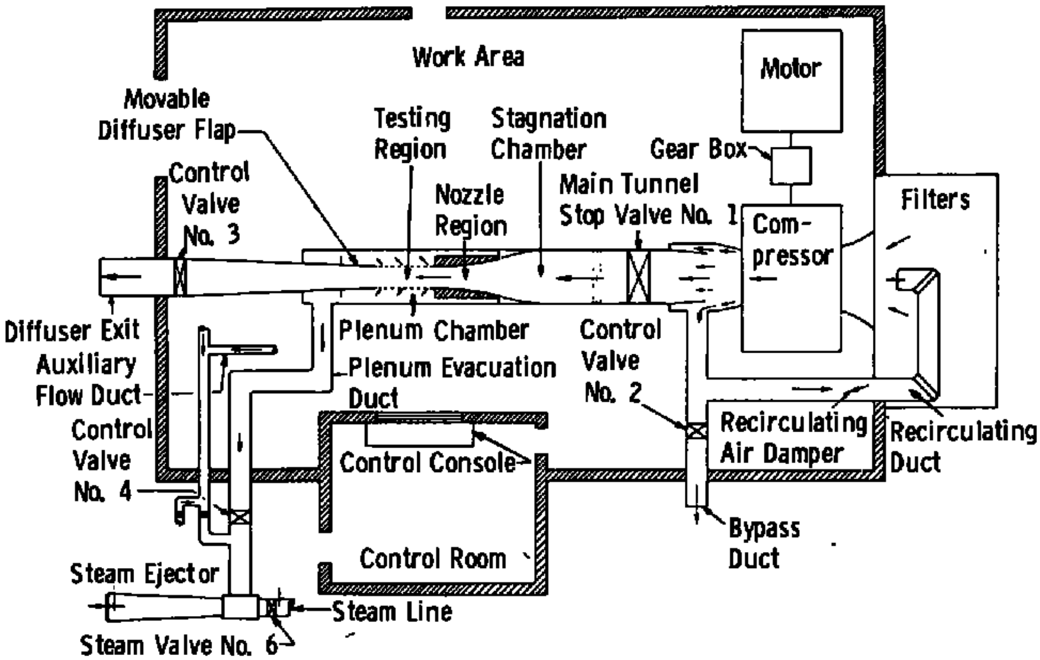

Figure 1. General arrangement of the AEDC Tunnel 1T.

2.2 TEST MODEL

To verify the optimization algorithm, a 3-degree-of-freedom model was designed and fabricated. The semispan model has a full span deflectable leading edge (A_1), a partial span deflectable trailing edge (A_2), and a deflectable horizontal tail (A_3). The control surfaces were remotely controlled by small hydraulic actuators, shown in Figs. 2 and 3. The model was mounted from a nonmetric reflection plane. The reflection plane was pedestal-mounted from the tunnel sidewall, and the fairings for the pedestal were used to shield the hydraulic actuator systems, which were metric, to the model. The model support is shown in Fig. 4, and the model installation is shown in Fig. 5.

2.3 INSTRUMENTATION

2.3.1 Tunnel Instrumentation and Data Reduction Systems

Tunnel 1T is equipped with a permanently installed, automatic data recording system. A PDP 11/20 computer normally provides for data acquisition, data monitoring, model pitch control, and online data reduction. Reduced data are displayed on a line printer, and a high-speed paper tape punch records and stores raw data for later offline analysis. The pressure data are measured with differential pressure transducers referenced to the tunnel plenum

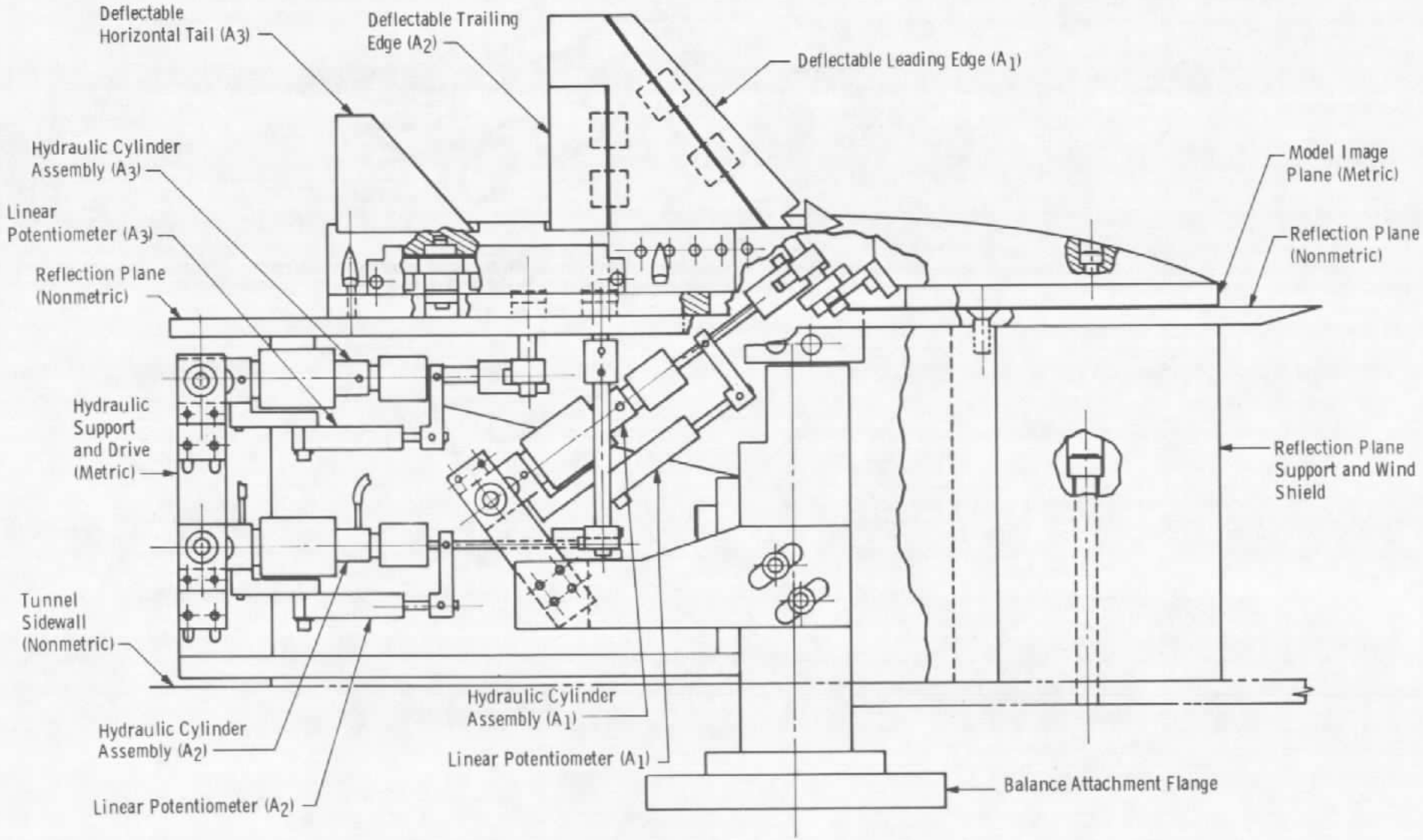

Figure 2. Model control system assembly.

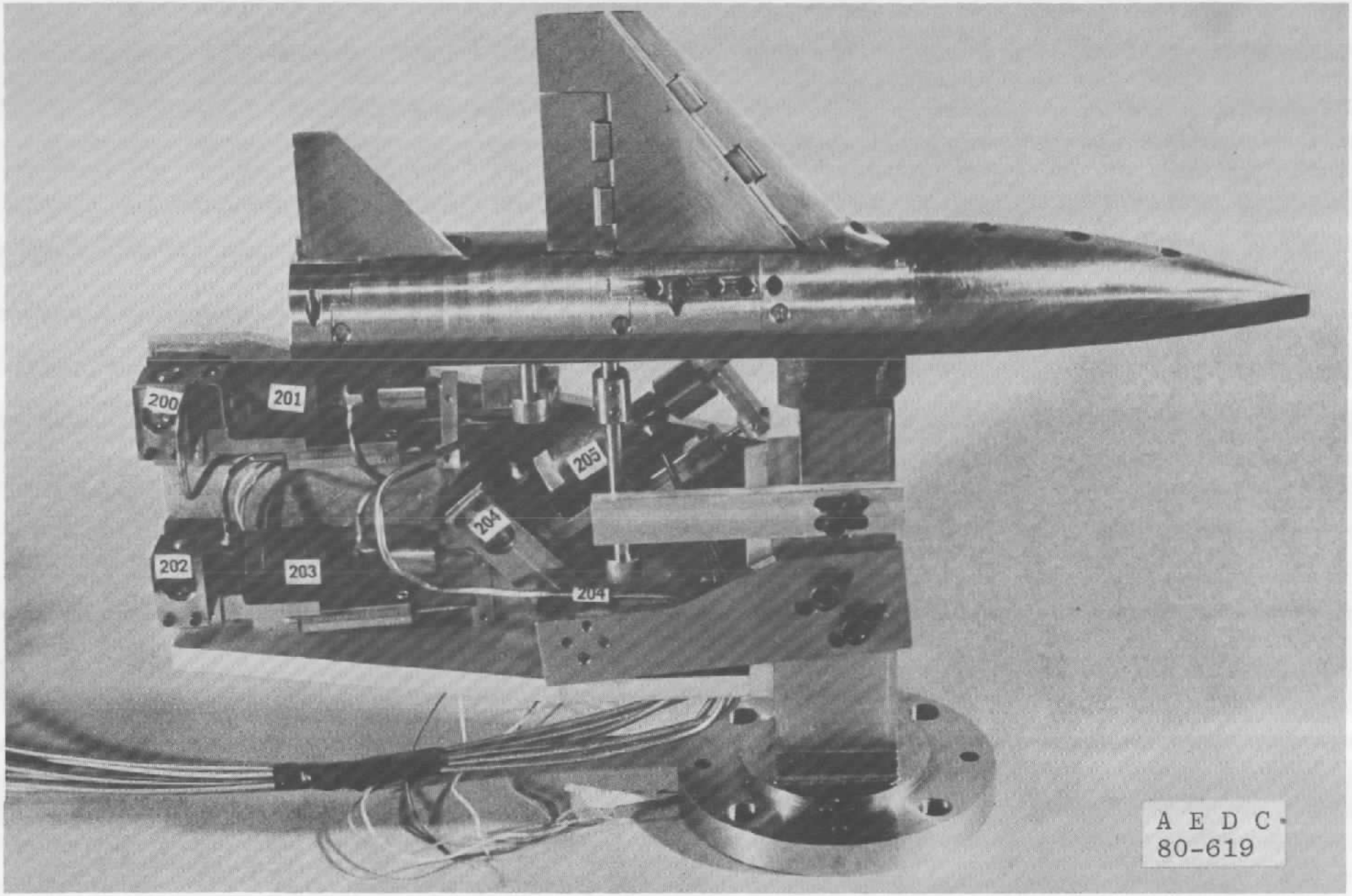

Figure 3. Photograph of model and control system assembly (metric).

pressure. Analog signals from the transducers are fed through a multiplexer, a switch gain amplifier, and an analog-to-digital (A/D) converter. The digital signal from the converter is processed by the PDP 11/20 computer.

During the present study the PDP 11/20 was interfaced with the PWT DEC System 10. This permitted the data reduction, optimization, and general management of the program to be performed by the DEC System 10, and the PDP 11/20 was used for data acquisition and model control. Four digital-to-analog converters (DAC) were installed on the PDP 11/20 for setting the model control surfaces. A terminal interfaced to the DEC System 10 was located in the Tunnel 1T control room for controlling the test. The line connecting the PDP 11/20 to the DEC System 10 was a telephone line using a driver and a receiver on each end. The

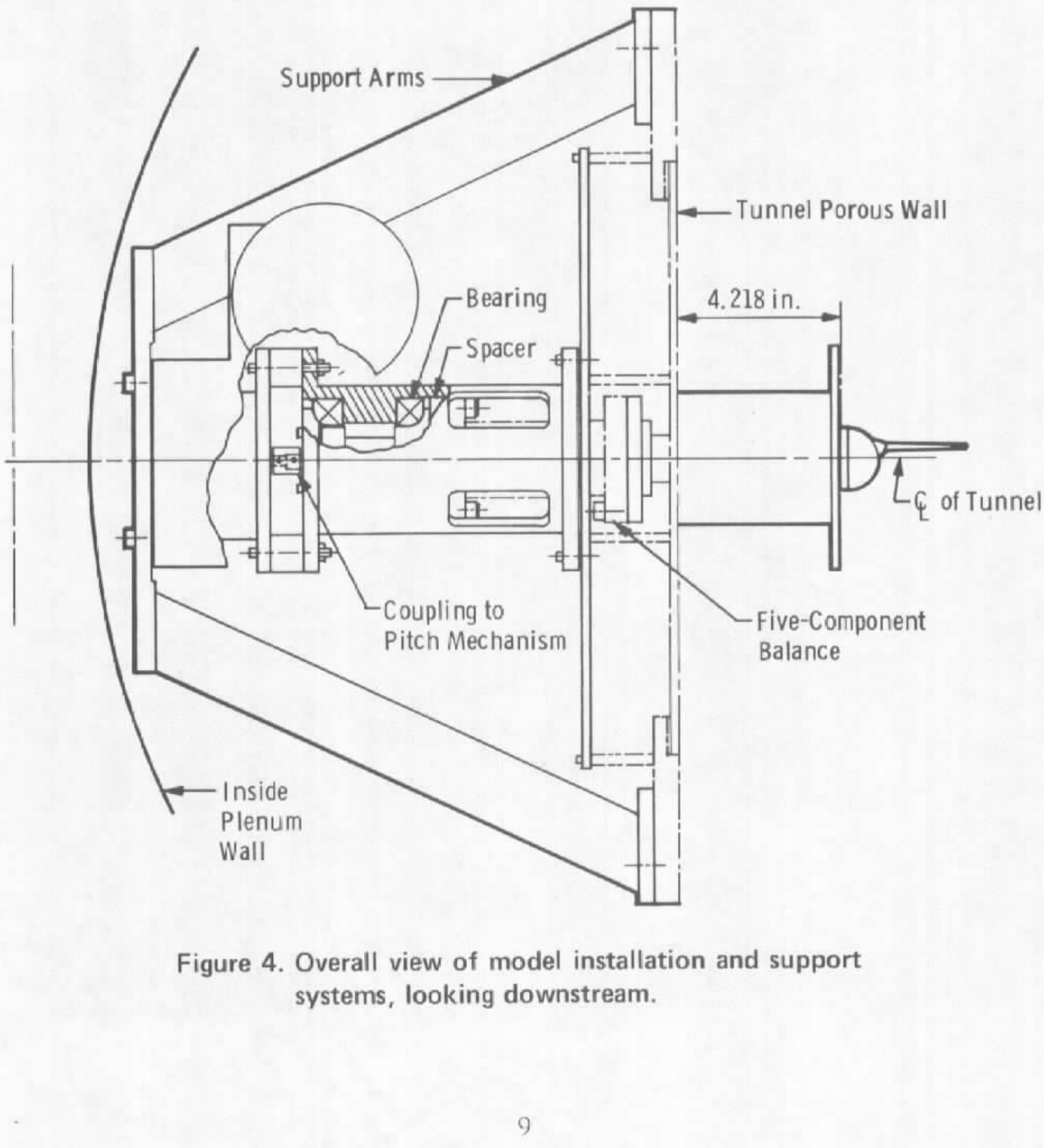

Figure 4. Overall view of model installation and support systems, looking downstream.

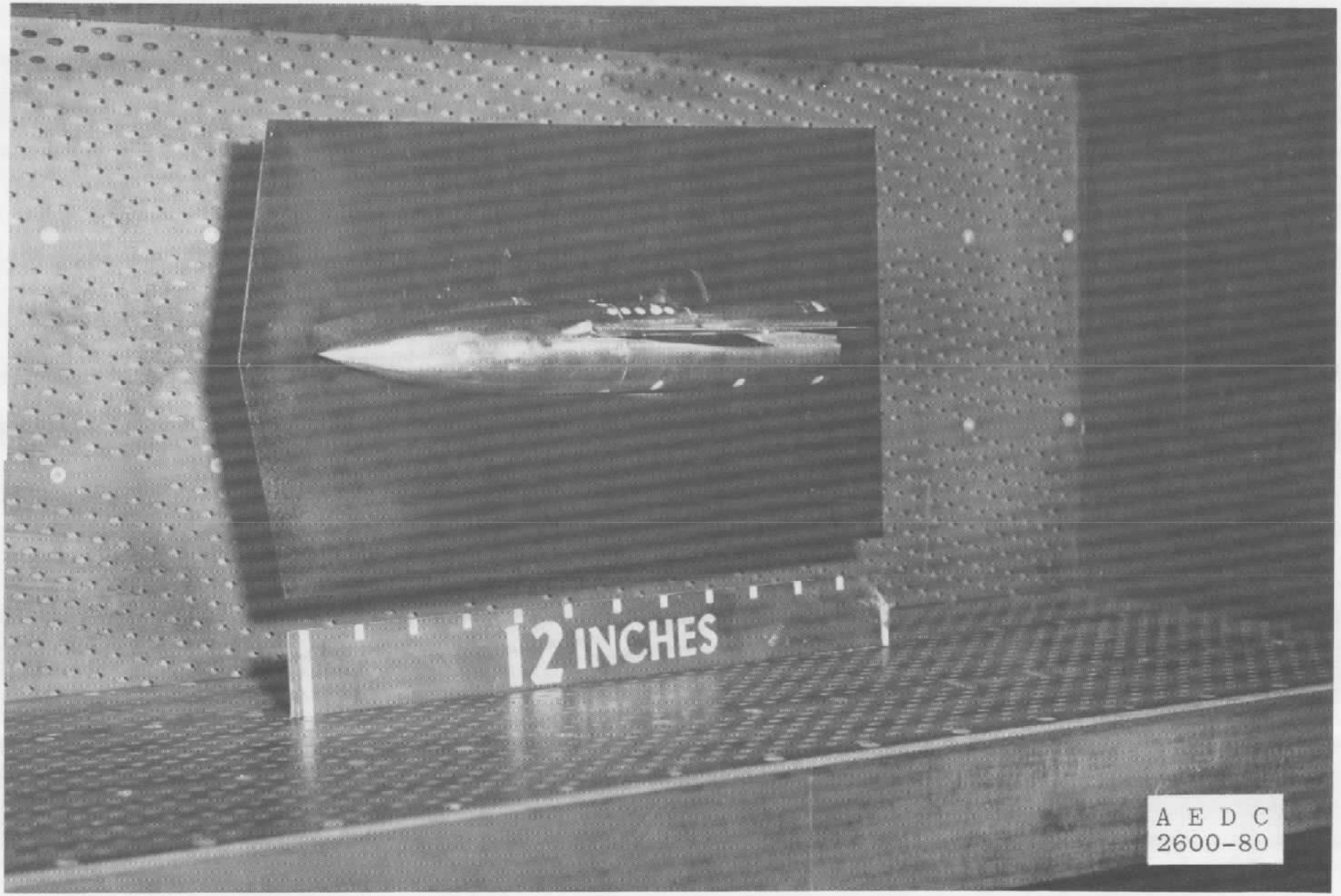

Figure 5. Model installed in Tunnel 1T.

maximum reliable transmission rate during the test was 1200 BAUD. However, because of the use of character echo to ensure the correct reception of the data, the actual rate of transmission was reduced to 600 BAUD. The slow transmission rate did affect the test program (see Section 3.1). A block diagram of the computer and model control systems is shown in Fig. 6.

2.3.2 Model Instrumentation

A five-component sidewall balance was used to measure the forces and moments on the model. The balance was calibrated as a standard balance. The calibration matrix was determined by applying the following maximum loads:

$$F_N = 80 \text{ lb}, F_y = 40 \text{ lb}, M_\ell = 72 \text{ in.-lb}, M_m = 680 \text{ in.-lb, and } M_n = 359 \text{ in.-lb}$$

with the probable 2-σ error for

$$F_N = 0.18, F_y = 0.34, M_\ell = 0.57, M_m = 0.83, \text{ and } M_n = 0.77$$

The balance was mounted to the model pitch mechanism as shown in Fig. 4.

The model control surface positions (A_1, A_2, and A_3) were measured using linear potentiometers (see Figs. 2 and 3), and the angle-of-attack position was measured with a synchro/digital converter.

2.4 HYDRAULIC AND CONTROL SYSTEMS

2.4.1 Hydraulic System

The hydraulic system was similar to the system used during the SOFT wing test of Ref. 3. The system consisted of three Moog® servohydraulic valves mounted on a four-port blocking valve. A 300-psi, pneumatically charged hydraulic accumulator was used to activate the blocking valve, and a 300-psi hydraulic supply was used to drive the hydraulic actuators in the model. A block diagram of the system is shown in Fig. 7.

2.4.2 Control System

Three servocontrol units were used for the test. The controllers were designed as self-contained, single-channel units that would provide easy calibration and monitoring of the complete control loop. The controllers provided excitation and signal conditioning for the

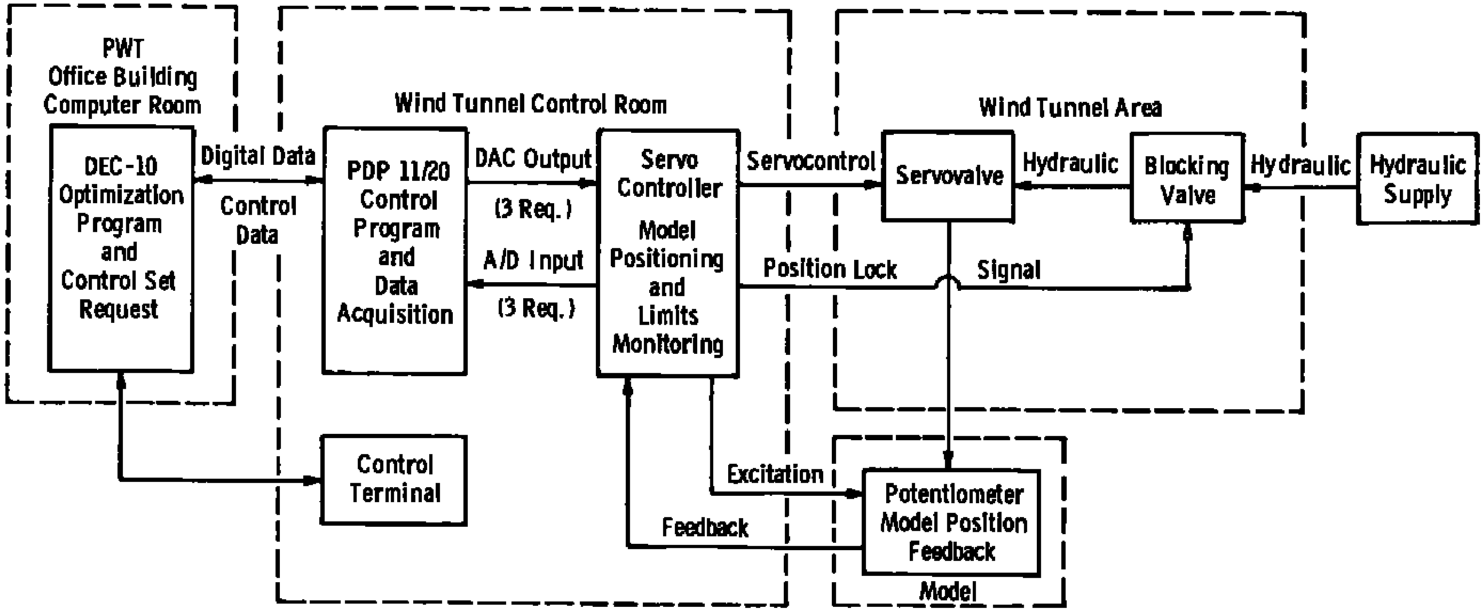

Figure 6. Interface of the model actuator control systems with computer systems.

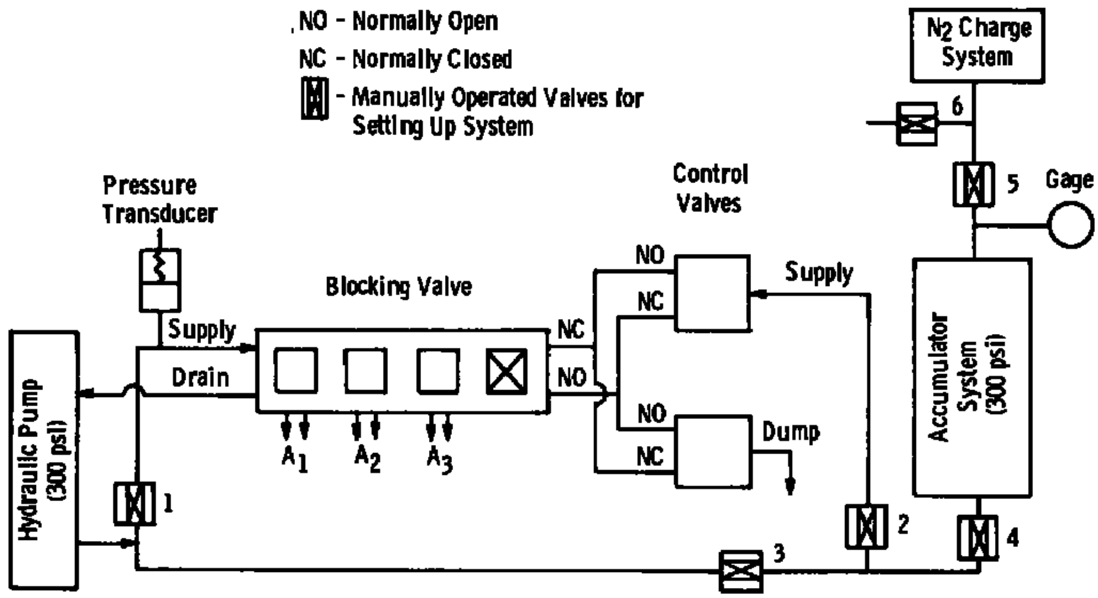

Figure 7. Hydraulic plumbing.

position feedback potentiometers as well as control to the Moog valves. The model limit protection was provided by an analog comparator in each controller that could detect travel limits and lock the model position with the blocking valves if the travel limits were exceeded. A complete description of the controllers is given in Ref. 3. The block diagram shown in Fig. 6 shows how the controllers interface with the computer and hydraulic systems.

3.0 PROCEDURE

3.1 TEST PROGRAM

The objectives of this study were twofold: (1) to check out the communication link between the test unit computer (PDP 11/20) and the facility computer (DEC System 10) and (2) to check out the modified optimization algorithm and determine its capability to optimize other aerodynamic parameters such as $C_{L_{max}}$ and L/D_{max}.

The communication link proved to be very slow, which made it expedient to limit the amount of data transferred over the line to the minimum required to meet the second objective. Since the SOFT wing study had adequately demonstrated the trimming capability of the algorithm, it was decided to hold the tail angle at a fixed minus 4 deg and not use C_m as an equality constraint. The inequality constraints consisted of the positive and negative

limits on the three model control surfaces and the model pitch angle (see Fig. 8). All optimization runs were made at a Mach number of 0.8. Each optimization tried was permitted to run only long enough to demonstrate convergence. When all of the constraints were satisfied and the program had gone through at least one minimization iteration, the optimization was usually terminated. No attempt was made to go through a complete optimization sequence to where the program will stop itself because of failure to improve the merit function.

The closed-loop testing techniques resembled those used during the SOFT-wing test of Ref. 3. Three general modes of operation were used during the test: (1) traditional table-driven positioning of any model control surface or model angle of attack to preselected attitudes (called parametric runs), (2) trimming of model to specified values of model lift coefficient (C_L) and model pitching moment (C_m) by adjusting model angle of attack and horizontal tail position, and (3) optimization of calculated aerodynamic parameters subject to constraints.

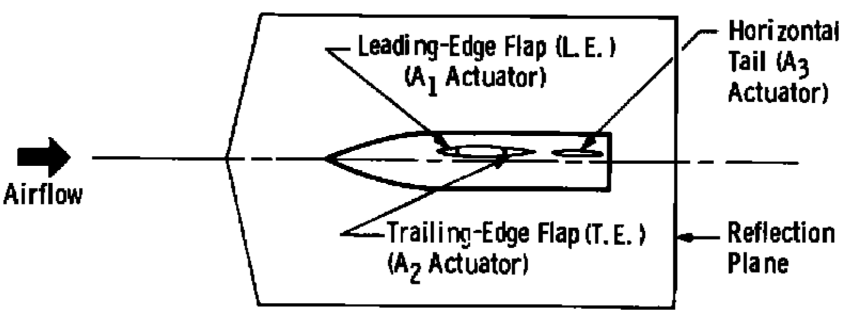

Sign Convention (As Installed, Upside Down)	Limits: Control Program, deg	Limits: Optimization Program, deg
L. E. Flap	- 5 to 15	-4 to 12
T. E. Flap	- 5 to 15	-2 to 12
Horizontal Tail	-10 to 12.5	-9 to 12
Angle of Attack	- 5 to 12.5	-4 to 12

Figure 8. Model control surface sign convention and program limits.

3.2 COMPUTER PROGRAMS

3.2.1 Control Program

A self-correcting control algorithm was developed in the PDP 11/20 to drive the model control surfaces to requested positions in accordance with position feedback volts from the servocontrollers. The requested positions were expressed in degrees. In the previous SOFT-wing test entries described in Refs. 1 through 3, the requested actuator settings were expressed in terms of feedback counts which varied over a range of 0 to 1,000; thus, any hardware adjustment would require considerable adjustment of instrumentation to ensure that 250 counts on all actuators represented the same model configuration. In the present test, a small hardware adjustment or actuator excursion was corrected by the curve fit of actuator position in degrees as a function of volts and the self-correcting control algorithm. Model angle of attack, horizontal tail, wing leading edge, and wing trailing edge were controlled by means of the same adjust-and-check algorithm for all modes of operation.

3.2.2 Data Reduction Program

Online data reduction, display, and tabulation were performed by the software modules resident in the PDP 11/20. The PDP 11/20 program had two basic types of operation: (1) as a stand-alone data acquisition, model control, data reduction, data presentation cycle that is mechanically initiated by depressing a data point start switch on the Tunnel 1T operating console (this type of operation was used for the parametric studies and trimming runs), and (2) as a slave in the master-slave relationship with the DEC System 10. The cycle of model control, data acquisition, data transfer to the DEC System 10 was initiated by a request from the DEC System 10. The data reduction and data evaluation were then performed by the DEC System 10, which would next request either another model control, data acquisition sequence, or a data acquisition and data presentation sequence. This type of operation was used for all optimization runs.

The data reduction module employed in the DEC System 10 was the same as that in the PDP 11/20. Because the rate of data transfer between the two computers was exceedingly slow, raw data rather than calculated data were passed from the PDP 11/20 to the DEC System 10 in order to minimize the number of variables transferred. It was necessary to have the data evaluation sequence for the optimization process done in the DEC System 10 rather than in the PDP 11/20 because of memory limitations in the PDP 11/20.

3.2.3 Optimization Program

The mathematical basis for the optimization program is given in Refs. 5 and 6. The optimization program of these references uses the gradient projection method with a Davidson-Fletcher-Powell (DFP) variable metric scheme for self-scaling. In conjunction with this procedure, transformations of variables are used to enforce independent variable constraints, and restoration steps are required to restore equality constraints that have become unsatisfied because of nonlinearities. The optimization program operates in two distinct modes: "incremental" and "simultaneous." Only the incremental mode is used during the initial iteration (and restart), during which each active control actuator and angle of attack is perturbed individually to generate gradient vectors of the merit function and active constraints. The number of incremental mode points per iteration depends upon the number of active actuators and on the number of times the perturbations are repeated to improve accuracy (termed "cycling").

After the incremental mode, the vector directions for either restoring the constraints or minimizing the objective function during the next iteration, depending upon whether any constraints were violated at the nominal incremental mode point, are calculated by the gradient projection algorithm. The next iteration begins with the simultaneous mode, during which all active actuators and angle of attack are advanced together in the direction obtained from the previous iteration through a sequence of up to 11 test points. The sequence is aborted if any of the constraints is violated by more than the prescribed tolerance. Upon completion of the stepping, the computer selects the "best" of the simultaneous mode points and then resets the model actuators and angle of attack to that configuration. The incremental mode is then repeated in preparation for the next iteration.

The optimization code used to support the last SOFT wing entry (Ref. 3) was revised to produce a code that will be more useful for future test applications. Modifications were made to eliminate the use of the DFP variable metric method described in Refs. 5 and 6. To utilize the DFP scaling matrix, it is necessary to evaluate second derivatives from information gathered from two consecutive minimization runs. In a test environment, practically all minimization runs are followed by a restoration run; therefore, the technique had limited practical application and was time- and space-consuming in the code. Modifications were also made to accommodate engineering unit parameters, rather than span counts. Program sequencing and algorithms were as defined in Ref. 3. Optimizations to maximize a merit function (e.g., $C_{L_{max}}$ and L/D_{max}) are accomplished by minimizing the negative of the merit function (e.g., $-C_L$ and $-L/D$). The definition of dependent functions, any of which could be selected as a merit function, is presented in Table 1.

Table 1. List of Dependent Functions

Function	Assignment	Definition
1	C_L	Lift Coefficient
2	C_D	Drag Coefficient
3	C_M	Pitching-Moment Coefficient
4	-L/D	-Ratio of Lift to Drag
5	$-A_1$	-Leading-Edge Deflection
6	$-A_2$	-Trailing-Edge Deflection
7	$-A_3$	-Horizontal Tail Deflection
8	-ALPHA	-Pitch Angle
9	A_1	Leading-Edge Deflection
10	A_2	Trailing-Edge Deflection
11	A_3	Horizontal Tail Deflection
12	ALPHA	Pitch Angle
13	$-C_L$	-Lift Coefficient

3.3 MODEL CONTROL SURFACE CALIBRATIONS AND LIMITS

The purpose of the model control surface calibration was to determine the relationship between model control surface position angles and the actuator positions and to determine the actuator position limits. The control surface sign convention and angular position limits are given in Fig. 8 along with the model angle-of-attack limits. Since the model control surfaces were very small, it was not possible to use a precision inclinometer to measure the surface angles. Therefore, a precision dial indicator was set up to read the surface position at a known distance from the control surface hinge line, and the control surface angular positions were then calculated using the readings from the dial indicator. The feedback voltage at the controller for the given surface angles was recorded and used for setting the model surface positions during the test. The calibration curves for each of the actuators are shown in Fig. 9.

The repeatability of the control surfaces and angle-of-attack data during the calibration, measured to readout, was found to be ± 0.10 deg. However, the inability to consistently stop the angle-of-attack drive system made it necessary to set the control tolerances to ± 0.2 deg.

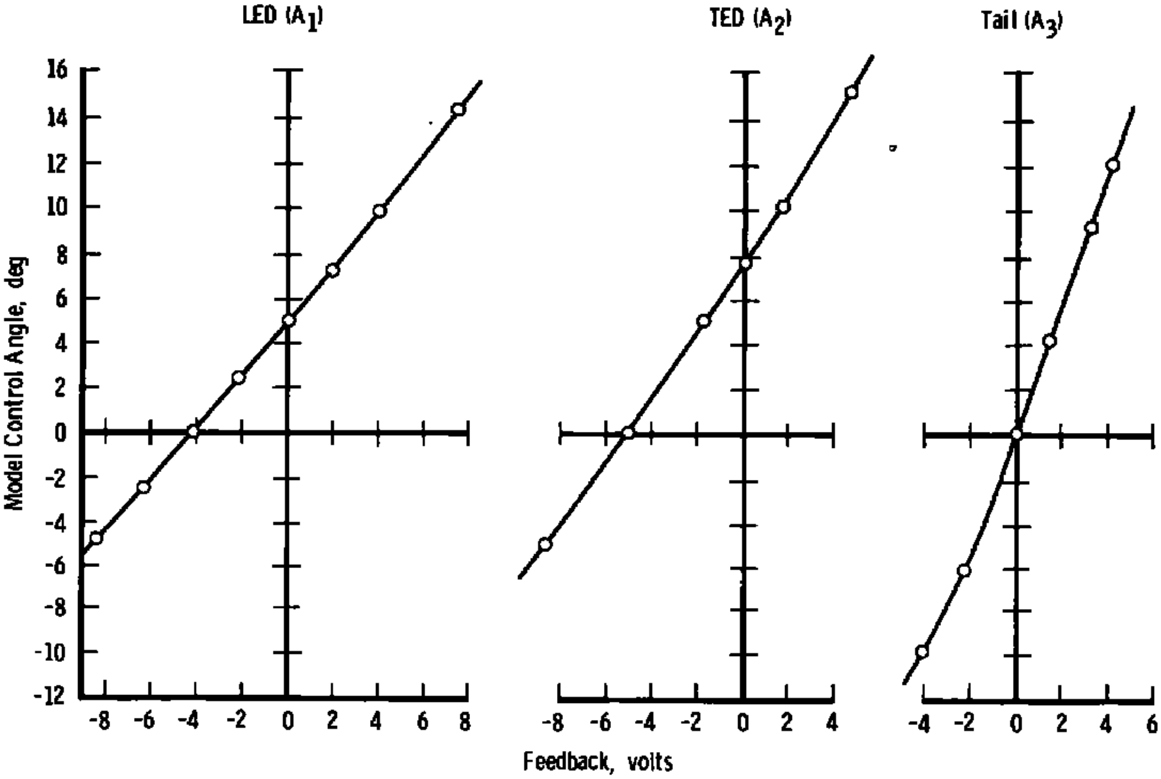

Figure 9. Actuator calibration.

4.0 RESULTS AND DISCUSSION

4.1 MINIMIZATION OF C_D

The first optimization was to minimize C_D with $C_L = 0.5$. The tolerance on the variation of C_L from the target value was specified as ± 0.01. This optimization was made to assure that the program revisions had not changed the effectiveness of optimizing for minimum C_D that had been demonstrated with the SOFT wing study. The summary of this optimization is shown in Fig. 10. The fourth point was the best point, with all constraints satisfied. Each optimization was stopped as soon as sufficient iterations had been made to assure that the algorithm was performing as desired. No attempt was made to let the program run until a true optimization was obtained. The convergence toward the optimum configuration and the lift/drag polar for the control settings from the best iteration are shown in Fig. 11.

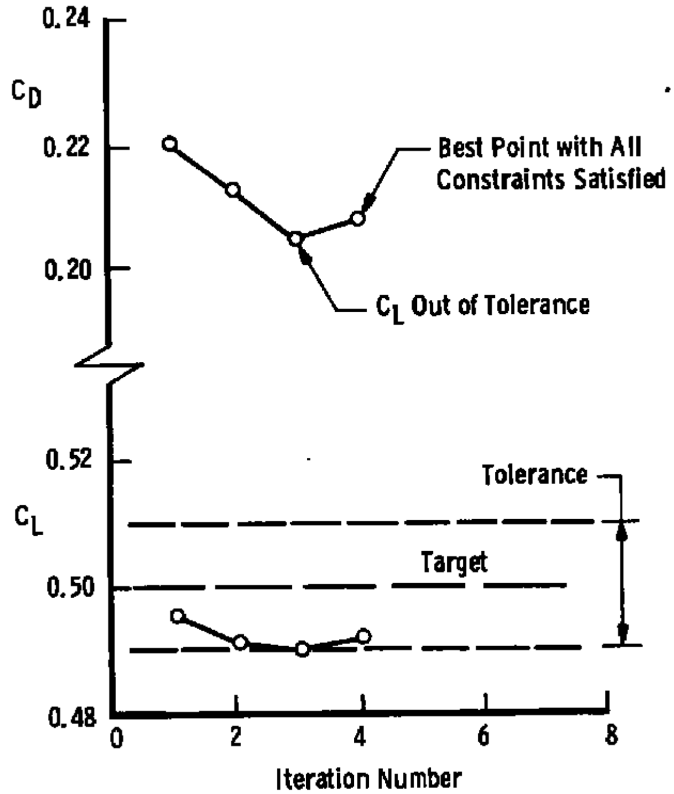

Figure 10. Optimization summary, minimizing C_D for C_L = 0.5, M_∞ = 0.8.

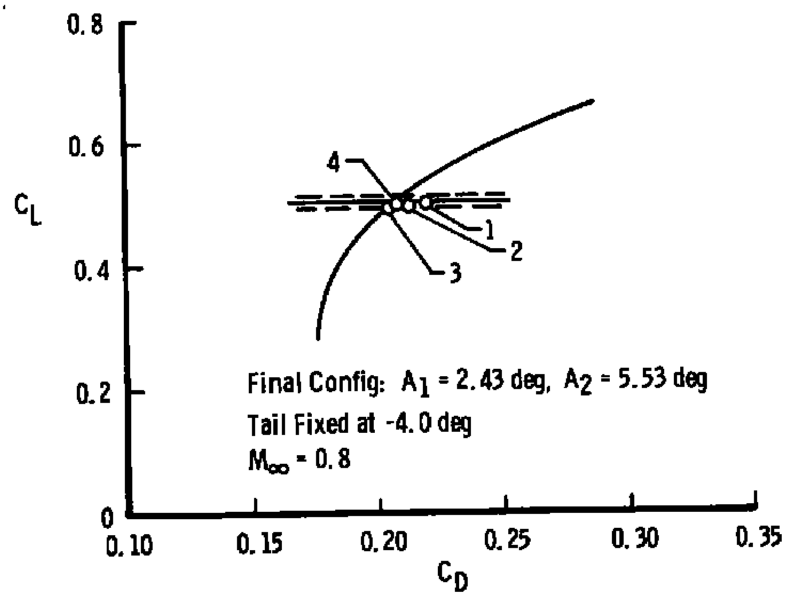

Figure 11. Convergence toward minimum C_D for C_L = 0.5 and lift/drag polar for resultant configuration.

4.2 MAXIMIZATION OF C_L

The second optimization was to maximize C_L with $C_D = 0.25$. The defining parameters for the computer program during this optimization are listed in Table 2. The objective function to be optimized is designated as $-C_L$ by the statement OBJ = 13 (13th dependent function in Table 1). Values of the other parameters are given for each of the 13 dependent functions. These include C (multiplier for activating equality constraints), CAN (specifies the type of constraint, if any, to be imposed), T (gives target or limiting constraint values), DEV (specifies the deviation by which the constraint can be violated before aborting a simultaneous mode search), TOL (assigns the tolerances to which each constraint must be restored), and ZNL (gives noise values for determining the smallest step sizes). Experience has shown that making DEV > TOL leads to faster convergence when constraints are activated. The tolerance on variation of C_D from the target value was set at ± 0.006.

A summary of this optimization is shown in Fig. 12. Four iterations were required to get within the required tolerance. Then the next two iterations were maximization iterations along the target value. This was somewhat surprising since the model pitch system would not set consistently with a tolerance of less than ± 0.2 deg and since all control parameters were set with the same constants box input; thus the model control surfaces had the same tolerance. The significance of the effect of the large tolerances is shown in Figs. 13 and 14. Figure 13 shows a restoration iteration (iteration 2). The solid symbols show the angles requested from the optimization program, and the open symbols show the angles that were set on the model. It can be seen that when the difference between one request and the next was within tolerance, the control computer would not change the control setting. This, of course, decreased the effectiveness of the optimization algorithm to fine tune the merit function. Another problem was the fact that the total drag was quite low with respect to the balance capacity; therefore, the drag coefficient was somewhat erratic. A maximization iteration (iteration 6), Fig. 14, shows that the same problem exists for this type iteration. However, in spite of the loose tolerances and somewhat erratic drag measurements, the optimization algorithm performed well and demonstrated the capability to maximize C_L. The convergence of the optimization and the lift/drag polar for the control settings from the best iteration are shown in Fig. 15.

4.3 MAXIMIZATION OF L/D

The final optimization was to maximize L/D with $C_D = 0.22$. The tolerance on the variation of C_D from the target value was again set at ± 0.006. The summary of the iterations is shown in Fig. 16. This optimization had trouble getting within tolerance.

Table 2. Summary of Optimization-Defining Parameters for Maximizing C_L with $C_D = 0.25$.

```
.DATE 10-FEB-81   PROJECT NO P32D-21C
*ARVIN/CALSPAN FIELD SERVICES, INC.
*AEDC DIVISION
*PROPULSION WIND TUNNEL
*ARNOLD AIR FORCE STATION, TENNESSEE
```

```
********************
*                  *
*   UNCLASSIFIED   *
*                  *
********************
```

TEST	RUN/PART	PROBLEM	MACH
0	1201	12	0.0000

PROBLEM DEFINING PARAMETERS

OBJ= 13.0 AMAX= 0.1200E+02

NUMBER	C	CAN	T	DEV	TOL	ZNL
1	0.0000E+00	0.0000E+00	0.0000E+00	0.4000E-01	0.1000E-01	0.1000E-02
2	0.1000E+01	0.1000E+01	0.2500E+00	0.2400E-01	0.6000E-02	0.3000E-03
3	0.0000E+00	0.0000E+00	0.0000E+00	0.2400E-01	0.6000E-02	0.3000E-03
4	0.0000E+00	0.0000E+00	0.0000E+00	0.2000E+01	0.1000E+01	0.1000E+00
5	0.0000E+00	-0.1000E+01	-0.1400E+02	0.4000E+00	0.2000E+00	0.3000E-01
6	0.0000E+00	-0.1000E+01	-0.1200E+02	0.4000E+00	0.2000E+00	0.3000E-01
7	0.0000E+00	-0.1000E+01	-0.1200E+02	0.4000E+00	0.2000E+00	0.3000E-01
8	0.0000E+00	-0.1000E+01	-0.1200E+02	0.4000E+00	0.2000E+00	0.5000E-01
9	0.0000E+00	-0.1000E+01	-0.4000E+01	0.4000E+00	0.2000E+00	0.3000E-01
10	0.0000E+00	-0.1000E+01	-0.2000E+01	0.4000E+00	0.2000E+00	0.3000E-01
11	0.0000E+00	-0.1000E+01	-0.9000E+01	0.4000E+00	0.2000E+00	0.3000E-01
12	0.0000E+00	-0.1000E+01	-0.4000E+01	0.4000E+00	0.2000E+00	0.5000E-01
13	0.0000E+00	0.0000E+00	0.0000E+00	0.4000E-01	0.1000E-01	0.1000E-02

INDEPENDENT VARIABLE NOISE LEVELS

0.3000E-01 0.3000E-01 0.3000E-01 0.5000E-01

INDEPENDENT VARIABLE PERTURBATIONS

0.4000E+00 0.4000E+00 0.0000E+00 0.4000E+00

However, it did get within tolerance on the sixth iteration. The optimization was stopped at this point because of a need to complete the test, and the optimization algorithm was showing convergence as expected. The convergence and the lift/drag polar for the control settings from the best iteration are shown in Fig. 17.

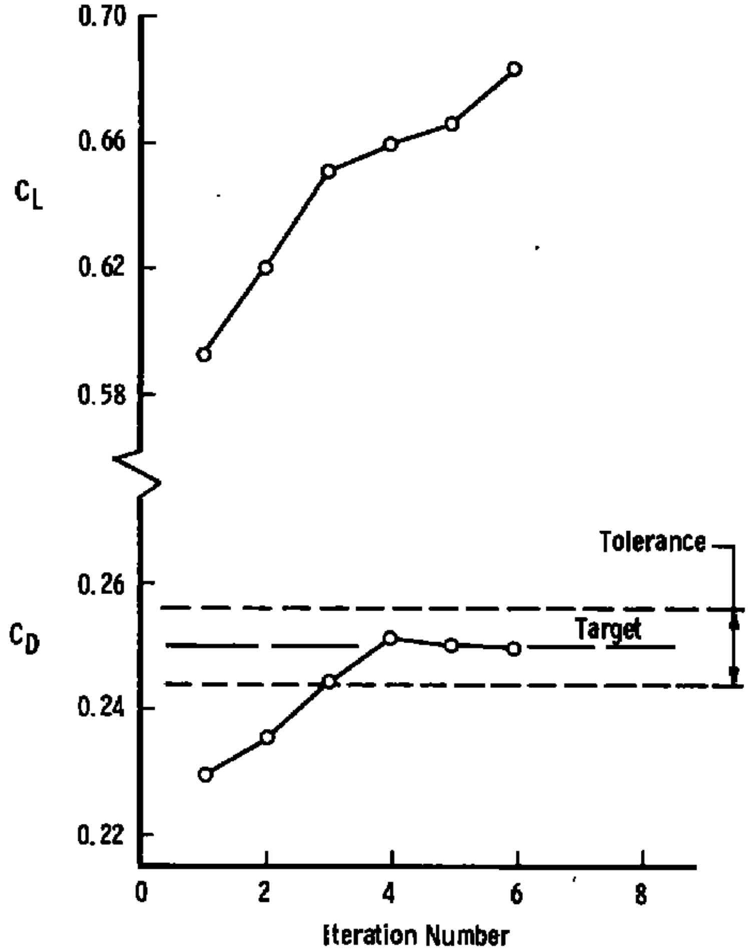

Figure 12. Optimization summary, maximizing C_L for C_D = 0.25, M_∞ = 0.8.

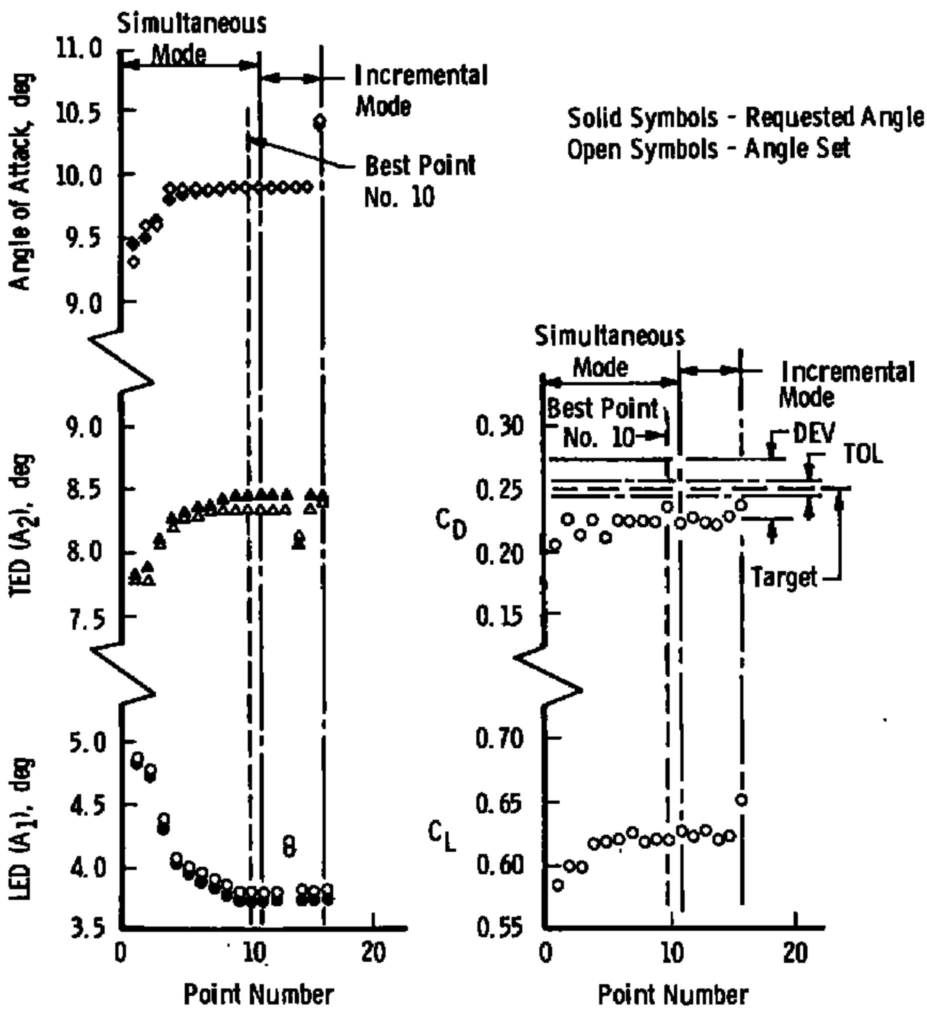

Figure 13. Restoration of C_D = 0.25 constraint during iteration 2.

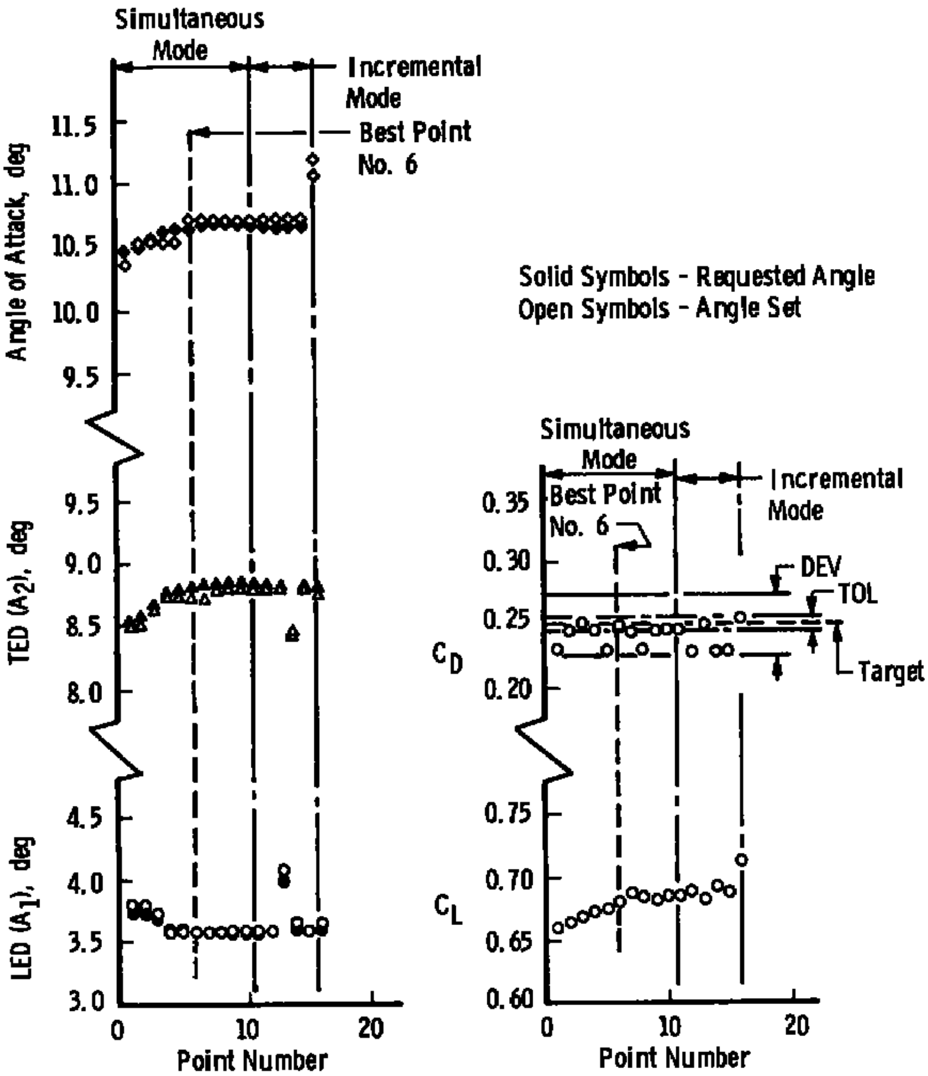

Figure 14. Maximization of C_L during iteration 6.

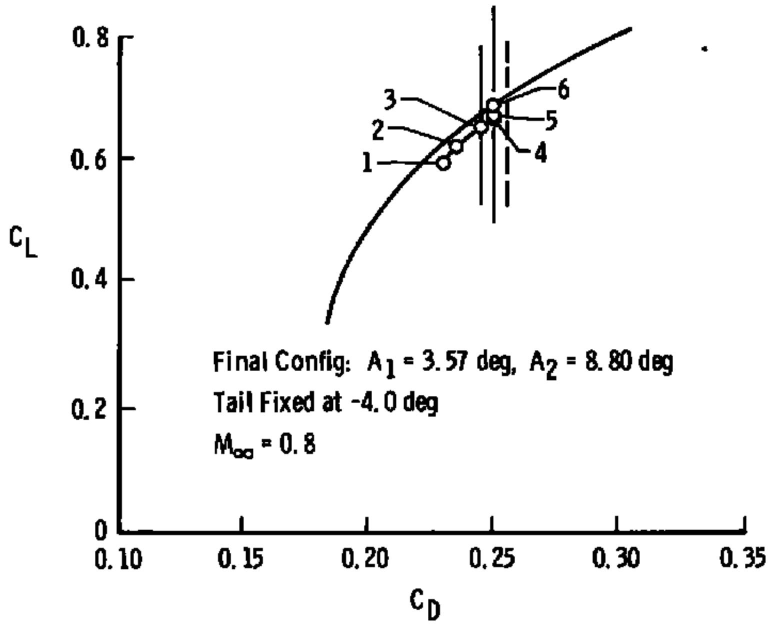

Figure 15. Convergence toward maximum C_L for C_D = 0.25 and lift/drag polar for resultant configuration.

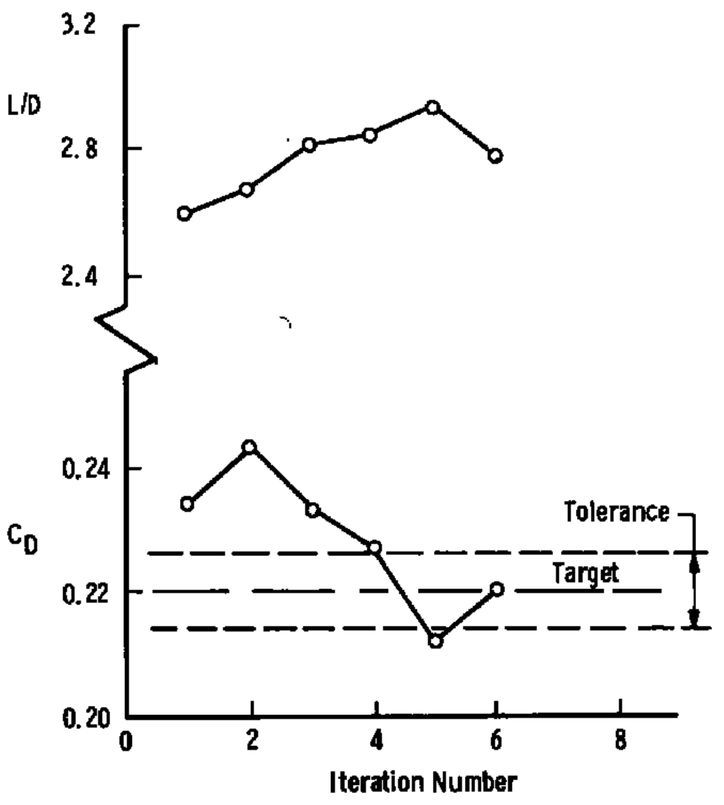

Figure 16. Optimization summary, maximizing L/D for C_D = 0.22, M_∞ = 0.8.

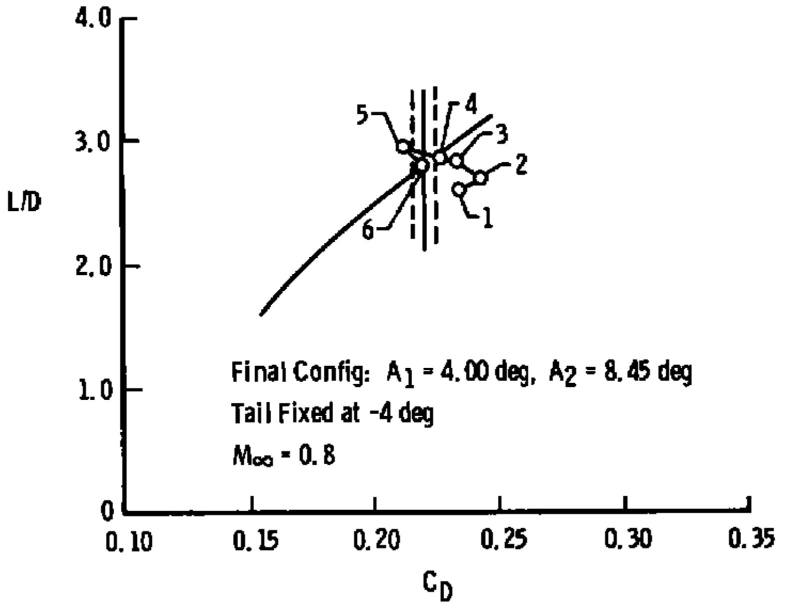

Figure 17. Convergence toward maximum L/D for C_D = 0.22 and lift/drag polar for resultant configuration.

5.0 CONCLUDING REMARKS

A wind tunnel test to verify a revised algorithm for optimization of aerodynamic parameters has been successfully completed in AEDC Tunnel 1T. The verification was made using a 3-degree-of-freedom model with a deflectable wing leading edge, wing trailing edge, and horizontal tail. All the verification runs were made at a Mach number of 0.8.

All major objectives of the program were accomplished in that:

1. The PWT facility computer (DEC System 10) and the Tunnel 1T computer (PDP 11/20) were interfaced to allow the DEC System 10 to be used for the optimization algorithm and overall program control. The PDP 11/20 was used for model and tunnel control as per instructions from the DEC System 10.

2. The algorithm was demonstrated to give convergent optimizations for all three of the problems attempted. These included (1) minimization of C_D for a specified C_L, (2) maximization of C_L for a specified C_D, and (3) maximization of L/D for a specified C_D.

The algorithm is now available for use at AEDC for any model test in which a parameter needs to be optimized subject to specified constraints. For such tests the model changes that affect the merit function and constraints must be remotely controlled, and these changes must be remotely measured. It should be noted that the computer communication problems associated with this test do not exist with the larger wind tunnels at AEDC where the actual system testing is performed. For these tunnels the communication links between tunnel computers and the facility DEC System 10 are parallel interfaces, and the slowest transmits at 320,000 BAUD as compared to the effective 600 BAUD available during this study.

REFERENCES

1. Levinsky, Ely S. and Palko, R. L. "Supercritical Tests of a Self-Optimizing Variable Chamber Wind Tunnel Model." Paper No. 21, NASA Advanced Technology Airfoil Conference, March 7-9, 1978.

2. Levinsky, Ely S. and Palko, R. L. "Semispan Wind Tunnel Test of a Computer-Controlled Self-Optimizing Flexible Technology (SOFT) Wing." Paper No. 78-786, AIAA 10th Aerodynamic Testing Conference, April 19-21, 1978.

3. Levinsky, Ely S. and Palko, R. L. "Test of an Improved Computer-Controlled, Self-Optimizing Variable Geometry Wing." AIAA Paper No. 82-0599, AIAA 12th Aerodynamic Testing Conference, March 22-24, 1982.

4. *Test Facilities Handbook* (Eleventh Edition). "Propulsion Wind Tunnel Facility, Vol. 4." Arnold Engineering Development Center, May 1981.

5. Levinsky, Ely S. and Schappelle, R. H. "Airfoil Optimization Utilizing a Remotely Controlled Flexible Model, Phase I: Low Speed Wind Tunnel Test." General Dynamics/Convair Technical Report CASD-NSC-74-007, 31 August 1974.

6. Levinsky, Ely S., Schappelle, R. H., and Pountney, S. "Airfoil Optimization Through the Adaptive Control of Camber and Thickness, Phase II: Transonic Wind Tunnel Test and Program Summary." General Dynamics/Convair Technical Report CASD-NSC-75-004, 30 September 1975.

NOMENCLATURE

A/D	Analog-to-digital converter
AMAX	Maximum allowable angle of attack (α)
A_N	Actuator (N = 1, 2, or 3)
BAUD	Data transmission rate (the number of times the state of a line changes per second)
C	Multiplier for activating equality constants (1 active, 0 inactive)
CAN	Candidate flag for specifying type of constraint (-1 inequality, 0 none, +1 equality)
C_D	Drag coefficient
C_L	Lift coefficient
C_m	Pitching-moment coefficient
DAC	Digital-to-analog converter
DEV	Maximum deviation allowable during simultaneous mode
F_N	Normal force
F_y	Side force
L/D	Lift-to-drag ratio
LED	Leading-edge deflection
M_ℓ	Rolling moment, in.-lb
M_m	Pitching moment, in.-lb
M_n	Yawing moment, in.-lb
M_∞	Free-stream Mach number
NC	Normally closed

NO	Normally open
OBJ	Objective function index
T	Target value and target vector of constraints
TED	Trailing-edge deflection
TOL	Tolerance for satisfying constraints during restoration
ZNL	Noise level used to determine step size during simultaneous mode